Predictive Modeling of Landslide Susceptibility in Soft Soil Canal Regions: A Focus on Early Warning Systems

Dang Tram Anh, Luong Vinh Quoc Danh, Chi-Ngon Nguyen*
Can Tho University, Can Tho City, Vietnam

***Abstract*—The Mekong Delta (MD) has suffered significant losses in land resources, economic damage, and human and property casualties due to recent landslides. An early warning system for landslides is a valuable tool for identifying the effectiveness and timely detection of changes in the soil to promptly determine solutions and minimize damage caused by landslides in an area. In this study, we apply a machine learning approach based on the Long Short-Term Memory (LSTM) algorithm to experiment with early warning of landslide events on soft soil in the MD. Horizontal pressure, the change in inclination angles of the sensor pile due to the soil mass sliding in both the x and y directions, and the warning levels are determined based on the deformation and displacement of the soil along the riverbank, considered candidate factors for inputs in the model. Data from the established sensor system is used to train the model, creating a training and testing dataset of 374,415 samples. The accuracy of the detection and classification threshold of the system is proposed to be measured using the average F1 score derived from precision and recall values. The optimal prediction results are gleaned from an observational window of 4 minutes and 30 seconds to project roughly 2 hours into the future. The validation process resulted in recall, precision, and F1-score stands at 0.8232 with a remarkably low standard deviation of about 1%. The successful application of this research can help identify abnormal events leading to riverbank landslides due to loading, thereby creating conditions for developing a reliable information system to provide managers with the ability to suggest timely solutions to protect the lives, property of residents and infrastructures.**

Keywords*—Landslide early warning; soft soil; Mekong Delta; long short-term memory

I. Introduction

Landslides represent a formidable global challenge, exerting a profound toll on economies, depleting natural resources, and tragically affecting human lives [1], [2]. Despite their localized occurrence, the ramifications of landslides extend far beyond their immediate vicinity, resulting in significant devastation to vital infrastructure elements such as roads, bridges, and power lines. This, in turn, leads to the distressing loss of land, homes, and, most tragically, human lives [3]. Vietnam in Southeast Asia bears witness to a history marked by a succession of natural disasters, including but not limited to floods, the encroaching threat of rising sea levels, shifts in climate patterns, coastal erosion, and the peril of landslides. Among the vulnerable regions, the Mekong Delta stands out, situated in the southern expanse of the country, densely populated yet perilously exposed to the caprices of nature. Its topographical identity is characterized by extensive low-lying stretches, intricately interlaced with an intricate network of rivers, canals, and verdant wetland areas, rendering it particularly susceptible to the forces of erosion and inundation.

The Mekong Delta region experiences a notable uptick in landslide occurrences, a trend that tends to peak during the rainy months. This phenomenon is intricately linked to the seasonal patterns of precipitation and the unique geological characteristics of the area. As moisture-laden rains saturate the soil and increase the weight and pressure on slopes, the propensity for landslides escalates. This heightened vulnerability underscores the need for vigilant monitoring and proactive mitigation measures to safeguard the natural landscape and its communities. According to the statistical data provided by the National Steering Committee for National Disaster Prevention and Control - Vietnam [4], until September 2023, there have been 558 locations of riverbank landslide within the area, resulting in a total affected and lost land length of over 740 km. Among these are 81 hazardous landslide sites and 137 high-risk landslide sites, causing damage to over 200 houses, residents' properties, and infrastructure worth thousands of billions of Vietnamese dong (VND).

Throughout the initial nine months of 2023, Can Tho City, situated among the thirteen provinces in the Mekong Delta region, bore the brunt of an alarming surge in landslides. This period witnessed an unsettling total of over 30 landslide incidents. These events led to injuries sustained by two individuals, the complete submersion of eight houses into the river, partial collapses, and grave impacts on 19 other residences. The cumulative length of the riverbank affected by these events totaled 1976 meters. Furthermore, the region has grappled with an escalating frequency of landslides in recent years, a trend partly attributed to the transformative impact of human activities and urban development encroaching upon riverine areas, thereby altering the natural landscape [5]. This surge in landslide occurrences has had far-reaching consequences, significantly and adversely affecting the lives of local residents and impeding the region's broader socio-economic development.

A preliminary assessment by domestic experts on the causes of erosion and instability of riverbanks and coastlines in the Mekong Delta region indicates that erosion at the base of the slope, saturated slopes after prolonged heavy rains or floods, and variations in groundwater levels are the primary factors contributing to slope instability along the riverbank [6], [7]. In addition to these long-term causes, the load of the structure, particularly the dynamic load induced by traffic,

*Corresponding authors.

can act as triggering factors for landslides [8], [9]. The complex relationships between landslide disasters and the factors that trigger them remain unclear. This complexity makes it challenging to analyze these mechanisms of landslides using simple algebraic equations [10]. Hence, predicting the ground's stress behavior and the soil mass's displacement along the riverbank becomes crucial and challenging.

The exploration of landslide risk assessment commenced in the 1970s [11]. Since then, propelled by advancements in modern statistical science and the advent of machine learning techniques, deep learning has become a vital tool in landslide research, particularly for landslide detection [12], [13], [14], [15]. While conventional approaches often treat landslide displacement prediction as a static regression problem, it is imperative to acknowledge that landslides are dynamic systems. The influencing factors and displacement conditions at one moment profoundly influence the subsequent moment. Thus, an effective landslide displacement prediction model should integrate susceptibility modeling, which considers the accumulation of variables over time.

The primary objective of this research is to present a predictive model for landslides utilizing advanced deep learning. The approach is rooted in the integration of input data, which encompasses variables such as soil pressure, incline in the x and y directions, alongside temporal factors. By harnessing machine learning algorithms, the primary aim of this work is to unravel the intricate interplay between these input parameters and their consequential impact on riverbank landslides. In the context of this study, a specialized form of recurrent neural network known as LSTM neural network was utilized to predict the progression of landslide events, extracting profound insights from time series data. This architectural framework excels in capturing complex patterns and temporal relationships in sequential data, providing favorable conditions for the development of a robust reduction framework. To facilitate the landslide prediction experiments, this study deployed a data collection system based on sensors. Through training on the gathered dataset, the model has demonstrated effective predicting capabilities for early warning of landslide phenomenon through training on the gathered dataset.

The underlying objective of the research is to study the performance of deep learning neural networks like LSTM to devise an early warning landslide system. The model is evaluated in term of accuracy on the dataset collected from the various experiments along the riverbank. In Section II we have discussed the related work. Section III explains the sources of collected dataset, the adopted methodology, the evaluation method and discusses the results in the study. Section IV is the conclusion of study.

II. Related Works

Recent machine learning and neural network breakthroughs have prompted extensive research, with CNNs being favored for their effectiveness in diverse applications. By utilizing neural networks, many researchers have developed landslide susceptibility maps and spatial modeling of landslides in highly prone mountainous areas using artificial neural networks [12], [16], [17], [18], [19], [20], [21]. Applying machine learning techniques along with GIS information [15], nonlinear spatial models have been created [22]. Neural Networks [23], [24], [25], [26], Boosted Regression Trees [27], [28], the Wavelet Transform model [29], [30] and Random Forest [31], [32], [33] are among the AI algorithms applied to tackle the intricate problems of landslide assessment. The Random Subspace Space Fuzzy Rule-based Classifier (RSSCE) is utilized to predict landslide occurrences based on the analysis of rainfall data triggered by heavy rainfalls in hilly areas [34], [35].

Research on landslide displacement prediction has indicated that utilizing deep learning on time series data, specifically the Long Short-Term Memory (LSTM) model, offers accurate forecasts [36]. LSTM's ability to capture historical information reduces the complexity of triggering factors, making it suitable for predicting landslide trends. Its performance in identifying these factors based on spatiotemporal sensor data demonstrates its superiority over other algorithms [37]. By extracting precise correlations between temporal and spatial data, LSTM has captured intricate time-dependent dependencies, outperforming traditional mechanical models [38]. The study in the Three Gorges Reservoir area, based on experimental mode decomposition and LSTM, has demonstrated superior accuracy compared to other static models in landslide displacement prediction [39]. Besides, [40] also proposes a novel coupled method using LSTM neural networks and support vector regression (SVR) algorithm, focusing on decomposing cumulative displacement into trend and periodic terms. The author introduces ensemble models based on SVR to optimize the combination of LSTM and SVR results, aiming for better accuracy in landslide predictions. The research on the mechanisms of damage and long short-term memory model for landslide prediction aims to address surface degradation phenomena, focusing on short-term impacts. The study emphasizes the effectiveness of LSTM in predicting landslide behavior and assessing damage based on joint distribution characteristics in building disaster prediction models [41]. These studies have applied the LSTM model based on various data such as rainfall, reservoir level, change in reservoir level, humidity, elevation, and displacement. The prediction results have observed that the prediction performance of the LSTM model is suitable and superior to static models like SVR, BP, SVM, ARMA, and even the dynamic Elman model.

Besides, combined models have been highly successful in fields such as flooding [42], [43] and drought [44], which has led researchers to explore ensemble modeling in landslide prediction as well. Risk analysis and forecast of landslide hazards using LSTM-RNN and DBA-LSTM models based on rainfall changes and water level variations have shown high accuracy [45], [46]. Researchers have used the original sequence of landslide displacement as input for combined machine learning models to predict the movement of landslides in steep slopes [47], [48], [49], [50]. The prediction of landslide movement in the major branches of the Three Gorges Dam area in China is carried out through combined models such as LSTM-TAR VMDstacked, LSTM-FC models, and LSTM models combined with Weighted Moving Average (WMA) using rainfall and reservoir water level data in each cycle with high accuracy [50], [51]. A prediction model for slope displacement based on the LSTM neural network and the Singular Spectrum Analysis (SSA) algorithm, using survey and geotechnical monitoring data, has significantly improved the model's performance in the dataset for predicting displacement within the next 24 hours

[52]. Landslides are likely to occur more frequently, along with climate change and the increasing surface loads caused by human activities.

In general, the conducted studies have been carried out in mountainous areas with a geological structure of loose rock. The primary factors causing landslide movements are mainly related to the permeability of the surface soil layer on the slope due to rainfall. In contrast to the riverbank landslides in the Mekong Delta, where the substrate is composed of alluvial deposits, young deltaic sediment, and riverbank soil with a predominantly geological structure of clayey soil, which is soft and weak. Additionally, factors contributing to riverbank landslides can arise from various causes: the inherently weak and saturated soil substrate with poor load-bearing capacity, subsurface erosion, changes in groundwater levels along the riverbank resulting in seepage flow, and human activities (such as construction and traffic), depicted in Fig. 2a. The studies on data collection systems based on modern sensor technologies or remote sensing techniques to generate databases for training landslide prediction models are presented in Table I and Table II. Thus, the need for early warning to assess the stability of slopes is becoming imperative [53]. Despite the extensive use of LSTM algorithms for landslide prediction in mountainous terrains with rocky geological structures, they have not been applied to predict riverbank landslides occurring in soft soil formations.

In this study, a new method to predict riverbank landslides using deep learning combined with data collected from sensors was proposed. To facilitate this, an Internet of Things (IoTs) - based sensor data collection and monitoring system have been implemented at the experiment sites along the riverbank within the Mekong Delta region. The collected data is used for training the LSTM machine learning algorithm to predict the possibility of riverbank slope instability for the purpose of early warning of riverbank landslides.

III. Methods

A. System Architecture for Predicting Landslides

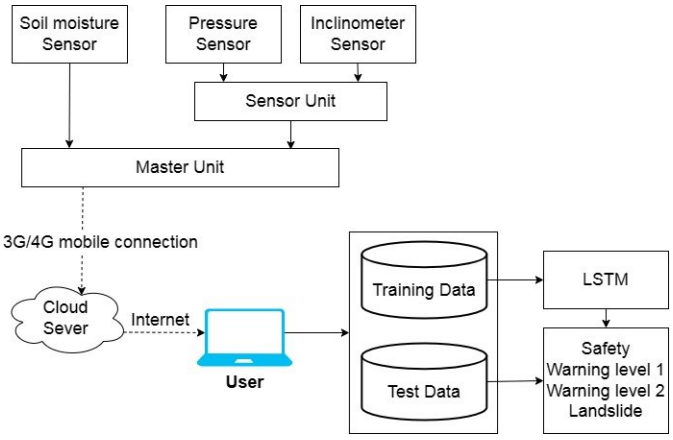

Fig. 1. System architecture for predicting landslides.

The architecture of the landslide prediction system is presented in Fig. 1. Our endeavor revolves around establishing a cutting-edge data collection framework focused on a diverse array of sensor devices. These instruments encompass a range of measurements, from monitoring soil moisture and inclination to gauging soil pressure. Central to this intricate setup is the Master Unit, a pivotal component acting as the central hub where these distinct sensors seamlessly converge to facilitate the precise acquisition of data. The Master Unit is a testament to seamless integration, meticulously designed to aggregate data from various sources with exceptional precision and efficiency.

In our commitment to ensure the accessibility and continuous availability of this data, we have dedicated substantial effort to engineer a robust data transmission mechanism. This designed system leverages the high-speed capabilities of 3G and 4G connectivity, enabling the collected data to be transferred from the Master Unit to our designated server. This data transmission process is characterized by its exceptional reliability and speed, forming an essential bridge that connects the physical realm of sensor data with the digital domain and ensures that this critical information is delivered promptly and with utmost accuracy.

The collected dataset undergoes a data preprocessing phase. This phase involves a blend of data cleansing, transformation, and normalization, all working in concert to ensure the data's integrity and suitability for subsequent analysis. A grid search method is employed on the training dataset to determine the appropriate number of layers of the LSTM method. The training dataset is split into two parts that comprise 80% and 20% of the dataset. The first part is used for training the model, and the second part is used to test the model's predictive ability. The crux of our methodology resides in utilizing deep learning architectures: LSTM. Our predictive framework relies on this algorithm model, which is predictable in time series within sequential data. The primary objective of this study is to forecast the warning level and landslide probability at time t, utilizing current time series data. This proactive approach significantly enhances the effectiveness of relocation efforts and minimizes potential damage in the aftermath of a landslide.

B. Experimental Setup for Data Collection System

In this work, to ensure consistency with the geological reality of the study, we excavated a channel (measuring $25m \times 3m$, with a slope ratio of $H = 0.5, V = 2$ on the banks of the Cai Sau channel in Can Tho city and tested the proposed system (Fig. 3). The geology at the research location is determined to be soft soil with the following physico-mechanical parameters: soil cohesion $C = 8.1kPa$, internal friction angle $\phi = 316'$, bulk weight $w = 1.571g/cm^3$, void ratio $e = 1.808$ and its initial water contents was 67%. The sensor pile is fixed at a distance of $0.1m$ from the channel bank edge (Fig. 4). The sensor node is composed of one Master unit and a Sensor unit. The soil pressure transducer is fixed on the sensor pile and inserted at a depth of 0.2 to 0.4 meters from the ground surface. The inclination sensor is compact (5 to $8mm$ in width and $10mm$ in length), installed in a waterproof plastic tube, and fixed on the sensor pile. The inclination sensor and soil pressure transducer are connected to the Sensor unit. The other item to be measured is soil moisture using a soil moisture sensor. This type of sensor is easy to use, plugged into the soil at a depth of $0.2m$ to observe and maintain the moisture of the canal bank slope in a saturated state throughout the

TABLE I. MONITORING SYSTEMS PROVIDE EARLY WARNING OF LANDSLIDES

Landslide warning system	System	Input data	Topographic characteristics of the study area
In the world			
One sensor node is the collection of three types of sensors that are displacement sensor, pore pressure sensor and moisture sensor [54].	Landslide early warning system (LEWS)	Rain-fall, pore pressure, moisture and displacement	Mountainous regions
The Infrastructure Node (IN), the Subsurface Node (SN) and the Low-Cost Chain Inclinometer (LCI) [55].	LEWS based on IoTs technologies such as micro-electro-mechanical systems (MEMS) sensors and the LoRa (Long Range) communication protocol.	Subsurface deformation and ground seepage-water levels	Mountainous regions
Tilt sensors and volumetric water content sensors [56].	LEWS – MEMS	The tilting angles and moisture content	Mountainous regions
The on- site monitoring and collection nodes are composed of one STM32L071RBT6 microprocessor and one STM32 microprocessor processes the sensor data acquired [57].	Real-Time Monitoring System of Landslide - LoRa.	Rainfall, displacement, tilt and acceleration	Mountainous regions
Pressure sensors and strain gauges measure water pressure and soil displacement respectively [58].	Landslide Early Warning Wireless Sensor Networks (LEWS - WSNs) Ultra-wideband (UWB)	Soil moisture, water level, soil inclination and temperature	Mountainous regions
Volumetric water content (VWC) and pore water pressure (PWP) [59].	Local landslide early warning system (Lo-LEWS)	The calculated safety factor (FS), the temperature, the precipitation, the VWC and PWP monitored were used as input dataset for a supervised machine learning algorithm	Mountainous regions
In Viet Nam			
The proposed system consists of six sensor nodes and one rainfall station [60].	Rainfall-induced landslide early warning (EWMRIL) - ZigBee	Soil moisture, PWP, movement status, and rainfall.	Mountainous regions

testing process. Then, the Sensor unit and Soil moisture sensor are connected to the Master unit. Measurement data will be transmitted to the Cloud server via 3G/4G mobile networks by the Master unit every 60 seconds. Solar power is used to provide energy for the sensor node.

The applied load is in the form of a strip load, simulating the load of the structure along the riverbank. The pressure exerted on the canal bank is created by sandbags placed on a steel plate with an area of 0.6m x 1.4m, arranged around the sensor pile with a distance of $0.2m$ as shown in Fig. 3. The canal bank in the experimental area was saturated with artificial continuous rainfall of 15mm/h. After filling the canal with water, the canal's water level was changed in combination with waves generated (by wave generators) to create a scour hole at the base of the slope as in Fig. 2. The strip load was gradually increased until the landslide occurred. Each load level was 3.5 kPa. Data on soil pressure, pile tilt angle, and soil moisture were recorded during the experiment.

Measurement data of inclination angle and soil pressure during the destructive deformation of the ground at the pile position are shown in Fig. 5, respectively. It can be observed that the landslide occurs in a relatively short time, only a few minutes since the mechanism of landslide is sudden deformation. Values of the inclination angle in the two directions, x y, differ in magnitude and time because the sensor pile moves along with the sliding ground mass.

C. Dataset

We performed testing at 45 sites. Each experiment lasted approximately seven days. The loading and data recording started 24 hours after embedding the sensor piles into the riverbank soil mass, with the load level increasing from 3.0 kPa to 4.5 kPa at each level. Each loading level was applied for continuous 11-hour intervals. An illustrative example of a measured data set is the horizontal soil pressure recorded during the second loading phase, which was 1.16 kPa. The X and Y tilt angles showed minor variations in the first 3 hours due to soil structure consolidating pressure, increasing soil compactness at the measurement site. Loading gradually increased at specified intervals until signs of soil failure became apparent. Such data recorded at 12:35:58 on December 19, 2022, as shown in Fig. 5, indicated a horizontal soil pressure of 1.9 kPa under an applied total load of 13.5 kPa. At 22:13:28 on

TABLE II. RESEARCH ON LANDSLIDES IN THE MEKONG DELTA

Research	Method	Results
Initial assessment on the causes of riverbank instability in Chau Thanh district, Hau Giang province [6].	Google Earth remote sensing images from 2006 to 2019 were used to assess the current status of riverside construction and erosion. The Analytic Hierarchy Process (AHP) was used to determine the impact levels of factors that cause riverbank instability. Using the AHP method and field survey can be extended to other areas in the Mekong Delta to analyze riverbank stability.	The survey and analysis results show that geology is the most affecting factor among the factors, and in combination with the encroaching construction of riversides to protection buffer areas, it creates the surcharge load reducing the stability coefficient of the riverbank. Besides, the curvature and flow velocity are also the causes of riverbed erosion and deformation, leading to an increase in the stiff slope which affects riverbank stability.
Analysis of factors affecting riverbank stability: case study at Cha Va river section, Vinh Long province [61].	Satellite images were loaded from Google Earth to analyze the current erosion of the river banks and the urbanization process along the river banks.	The integrated effects of soft soil, water level fluctuation, wave load, and surcharge loads is found to be the cause of instability of the Chavas river bank.
Assessment of the situation of landslides and sedimentation in the coastal area of Ca Mau and Bac Lieu province from 1995-2010 using remote sensing and GIS technology [62].	Research using remote sensing images Landsat	Assess shoreline changes erosion or deposition processes
Monitoring developments in Cu Lao Dung's coastline using remote sensing image analysis technology [63].	Multispectral Landsat images were utilizad for the analysis	Analyze erosion and deposition locations with specific values
Monitoring erosion and accretion situation in the coastal zone at Kien Giang province [64].	The study applied Normalized Difference Water Index (MNWI) method and water level extraction using LANDSAT imagery from 1975 to 2015 for highlight the shoreline.	Analysis was identified erosion and accretion areas based on shoreline changes and land use influenced by landslides and deposition

the same day, the horizontal soil pressure measured was 2.11 kPa and showed a decreasing trend. Subsequently, continuous changes in soil pressure and sensor pile tilt were observed, accompanied by the appearance of cracks on the canal bank, as shown in Fig. 4 (small cracks visible). This indicated that the soil had reached its ultimate limit state. By 23:34:58 on December 19, 2022, when the horizontal soil pressure reached 2.13 kPa, an additional loading level was applied, raising the total load to 18 kPa. The horizontal soil pressure and tilt angle remained relatively stable for about 1 hour and 30 minutes, while monitoring revealed the gradual expansion of cracks. Simultaneously, the soil pressure data showed a rapid decrease, and the tilt angle of the sensor pile experienced a sudden significant change. Finally, the canal bank slope completely slid after the horizontal soil pressure reached its peak value of 2.5 kPa. Data measured from sensors will be saved as data files on the memory card. Then, the Master device will scan the memory card and transmit the data files to the Cloud server. Users can download the measured data for analysis and real-time observation through the Web server. First, the dataset "landslide monitoring.csv" was downloaded. The monitoring dataset includes date and time, soil pressure, soil moisture, and inclination angles due to soil movement and landslides. Data was collected at one-second intervals throughout the loading experiment until the landslide occurred. We can use this data to address the prediction issue for the next two hours based on changes in ground pressure and soil displacement in the preceding hours. Next, the data was labeled and categorized according to warning levels. Then, the data was transformed into a supervised learning problem. We normalized the data for model training using a 30-second sliding window approach. After reprocessing, we obtained 374,415 samples, split into a training set comprising 70% (262,090 samples) and a test set comprising 30% (112,325 samples). The soil moisture content in the experimental conditions was always saturated; thus, this value was not included in the input dataset. There were three input variables: ground pressure (p), X-axis inclination angle (x angle), Y-axis inclination angle (y angle), warning level, and warning label arranged in 5 columns in the input data table.

D. Warning Thresholds

The calculated ultimate bearing capacity of the soil foundation using the finite element method based on geological parameters at the experimental site was determined to be 20.61 kPa. The analysis results of the finite element model under external loading show: (1) when the soil stress is below 40 percent of the ultimate bearing capacity, the soil remains in a safe state; (2) when the soil stress reaches a ratio below 70 percent of the ultimate bearing capacity, the soil starts deforming and consolidating; (3) similarly, when the ratio increases to 80 percent, the soil shows significant deformation and displacement; (4) finally, when this ratio exceeds 80

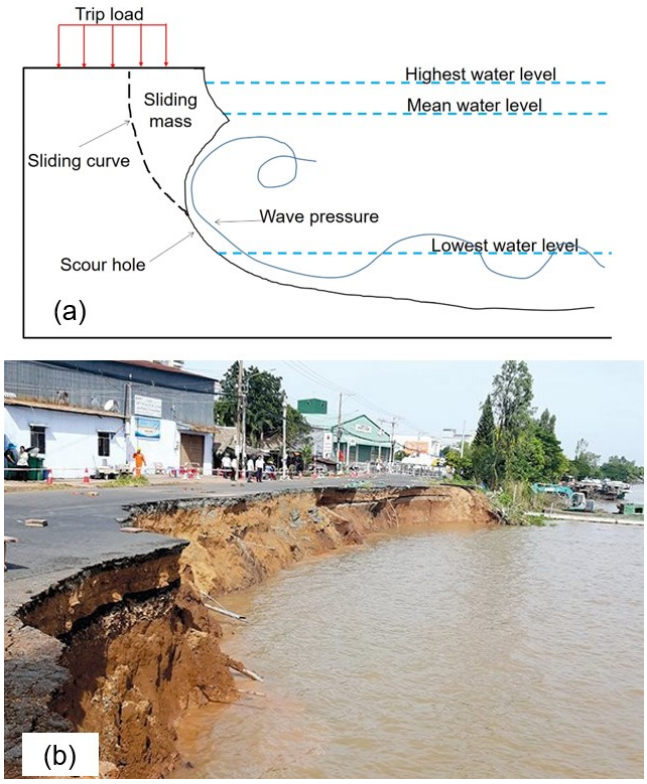

Fig. 2. Riverbank landslide: (a) Diagram of the main factors contributing to slope deformation; (b) Landslide submerges a section of national highway 91 into the hau river in an Giang province, Vietnam [65].

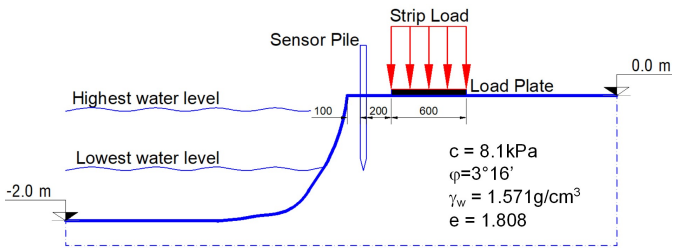

Fig. 3. Dimensions of the experimental canal.

Fig. 4. Photo taken at the experimental site.

TABLE III. PRESSURE RATIO VALUES TO DETERMINE THE WARNING THRESHOLDS

Soil pressure factor	Displacement	Level of warning
k $\leq$ 40%.qult	-	Safety
40%.qult <k $\leq$ 70%.qult	Narrow oscillation angle	Warning level 1
70%.qult <k $\leq$ 80%.qult	The oscillation angle gradually widens	Warning level 2
k >80%.qult	Sudden fluctuation in the oscillation angle	Landslide

percent, the analysis results indicate complete deformation and destruction of the soil. The analysis results using the numerical method extracted from Plaxis software are presented in Fig. 6, 7, 8, 9 with the surveyed load levels of 30%, 63%, 82.5% and 99.5% of the ultimate bearing capacity, respectively. Fig. 9 clearly shows the sliding curve of the riverbank soil mass (highlighted in orange) and the failure strain area (highlighted in red). The results of soil pressure values in the horizontal direction and displacement obtained from the measurement system showed similarities in pressure ratios with the model analysis results. Therefore, we have proposed pressure ratio values to determine the warning thresholds as shown in Table III below, where q_{ult} is the ultimate bearing capacity of the ground.

E. Long Short-Term Memory

The architecture of an LSTM neural network is explicitly designed to handle sequential data, making it a powerful tool for tasks like time series prediction, natural language processing, and more. At its core, an LSTM network comprises individual LSTM cells that work together in a chain-like structure (see Fig. 11). Each LSTM cell (see Fig. 10) contains three main gates: the Forget Gate, the Input Gate, and the Output Gate, along with a Candidate Gate. These gates, implemented using a combination of activation functions and weights, control the flow of information through the cell. The Forget Gate determines what information to discard from the previous cell state. The Input Gate decides what new information to store in the cell state, and the Output Gate regulates what information to expose to the output. This ar-

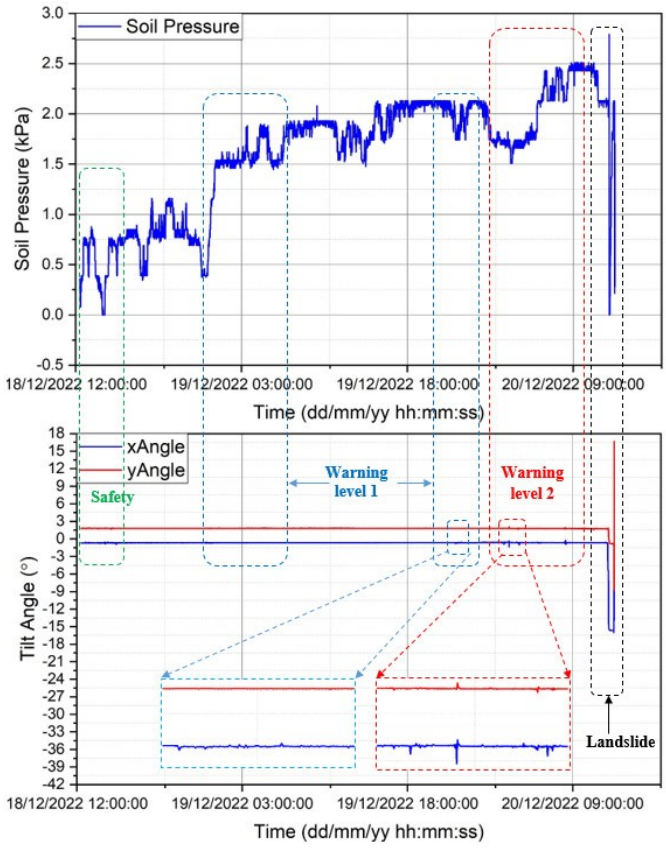

Fig. 5. A specific illustration of warning thresholds based on soil pressure and inclination displacement data of sensor piles.

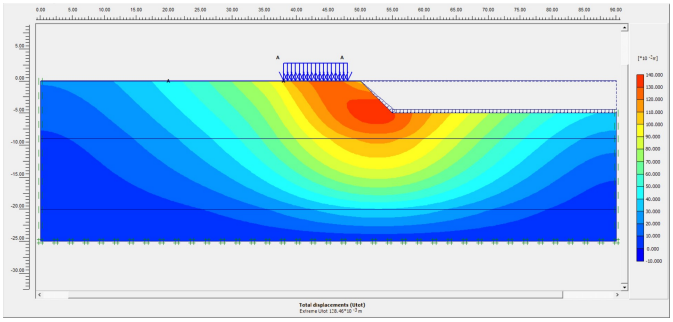

Fig. 6. The total displacement result at the load level q=6kPa.

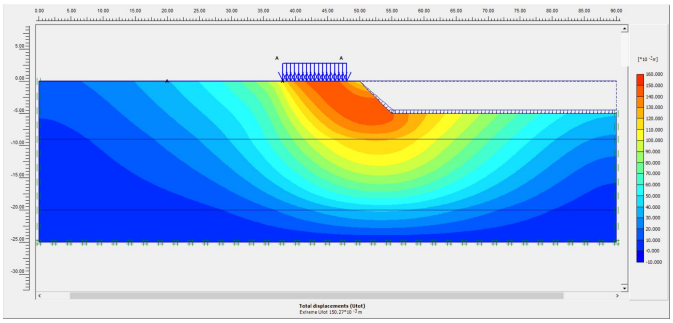

Fig. 7. The total displacement result at the load level q=13kPa.

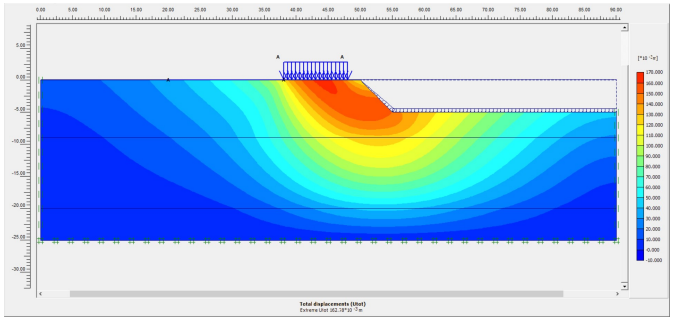

Fig. 8. The total displacement result at the load level q=17kPa.

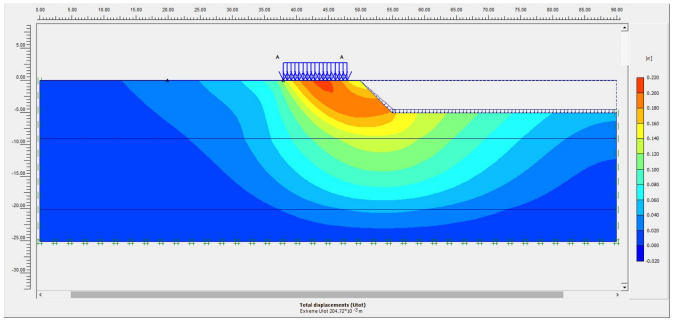

Fig. 9. The total displacement result at the load level q=20.5kPa.

chitectural design enables LSTMs to effectively capture long-term dependencies in sequential data, addressing the issue of vanishing or exploding gradients often encountered in standard RNNs.

The approach with LSTM models for landslide prediction represents a significant stride in harnessing advanced technology for geohazard mitigation. LSTM, a specialized form of recurrent neural network (RNN), excels in handling sequential data, making it particularly well-suited for predicting time-dependent variables associated with landslides. This is paramount in regions prone to geological instability, where timely warnings are crucial for safeguarding lives and infrastructure. One critical strength of LSTM models is their ability to capture intricate temporal dependencies and patterns within time series data. By incorporating memory cells that can retain and update information over time, LSTMs excel in modeling sequences characterized by long-term dependencies. This dynamic memory retention mechanism empowers the model to discern subtle shifts in environmental factors leading to a potential landslide event. Consequently, LSTM-based predictive models stand at the forefront of cutting-edge geotechnical research, offering a promising avenue for enhancing early warning systems and ultimately minimizing the impact of landslides on vulnerable communities.

The equations for an LSTM cell are as follows. In these equations, x_t represents the input at time t, h_t represents the hidden state at time t, c_t represents the cell state at time t, and f_t, i_t, g_t, and o_t represent the forget gate, input gate, cell gate, and output gate respectively.

1) Forget Gate:

$$f_t = \sigma(W_f \cdot [h_{t-1}, x_t] + b_f)$$

2) Input Gate:

$$i_t = \sigma(W_i \cdot [h_{t-1}, x_t] + b_i)$$

3) Candidate Cell State:

$$g_t = \tanh(W_c \cdot [h_{t-1}, x_t] + b_c)$$

4) Update Cell State:

$$c_t = f_t \cdot c_{t-1} + i_t \cdot g_t$$

5) Output Gate:

$$o_t = \sigma(W_o \cdot [h_{t-1}, x_t] + b_o)$$

6) Hidden State:

$$h_t = o_t \cdot \tanh(c_t)$$

Here,

- σ represents the sigmoid activation function.
- $\tanh$ represents the hyperbolic tangent activation function.
- W_f, W_i, W_c, and W_o are weight matrices specific to the forget gate, input gate, cell gate, and output gate, respectively.
- b_f, b_i, b_c, and b_o are bias vectors associated with the respective gates.

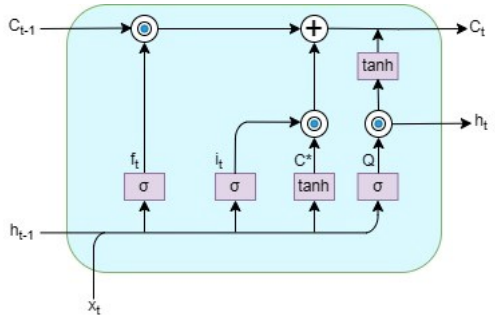

Fig. 10. The LSTM cell operation.

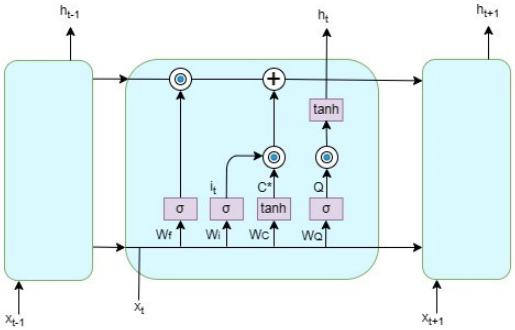

Fig. 11. Structure of LSTM.

F. Landslide Prediction with LSTM

LSTM networks resolve the vanishing gradient issue that hinders traditional RNN training by utilizing a memory cell capable of retaining information over extended durations. This quality makes them highly effective for modeling time series sequences, a crucial aspect in predicting landslides due to their complex temporal nature influenced by various factors.

The dataset gathered from 45 experimental points is vital for implementing the LSTM algorithm in predicting landslide warning levels. This extensive time series monitoring dataset captures a multitude of critical attributes, including ground pressure (p), the X-axis inclination angle (x angle), the Y-axis inclination angle (y angle), and the respective warning levels recorded at various experimental sites situated along the banks of Rach Cai Deep River. It's important to note that this dataset was meticulously collected at 30-second intervals, a frequency maintained throughout the loading test, persisting until a landslide event occurred. To formulate the predictive challenge effectively, we have stratified it into four levels: safety, warning level 1, warning level 2, and landslide. The very essence of this endeavor is rooted in the comprehensive time series data collected in the context of six scenarios. The particulars of these six distinct experimental scenarios are elucidated in depth in the experimental results section.

Furthermore, our experiments extend beyond mere data collection, encompassing the proactive prediction of landslide levels. This predictive process spans specific time intervals, specifically after 2 hours, 2.5 hours, 2.7 hours, 4.3 hours, 4.8 hours, and 5.5 hours post-initiation. This time horizon is of particular significance, representing a window during which strategic asset relocation can effectively mitigate the potential loss of valuable assets and infrastructure. For training and evaluating the LSTM model, the entire dataset is thoughtfully partitioned into two subsets. A substantial 70% of the data is designated for training, with the remaining 30% preserved for testing and validation. This partitioning strategy ensures the robustness and accuracy of the model's performance, affirming its capacity to effectively predict landslide warning levels under diverse temporal and environmental conditions.

G. Evaluation Method

In multiclass classification, the performance of a classification model is typically evaluated using various metrics to assess its accuracy and effectiveness in classifying data into multiple classes. The evaluation metrics used include accuracy, precision, and recall [66]. The F1 score is the harmonic mean of precision and recall, representing a balanced average between accuracy and recall [19], [67]. It ranges between 1 and 0. The highest possible value of F1 is 1.0, and an F1 score approaching 1 signifies perfect precision and recall, indicating high confidence and reliability of the algorithm in predicting landslide warning levels [68]. Detailing the indices presented in the documents [69], [70]. Common evaluation metrics include:

$$\text{Accuracy} = \frac{\text{Number of Correct Predictions}}{\text{Total Number of Predictions}} \quad (1)$$

$$\text{Precision} = \frac{\text{True Positives}}{\text{True Positives + False Positives}} \quad (2)$$

$$\text{Recall (Sensitivity)} = \frac{\text{True Positives}}{\text{True Positives + False Negatives}} \quad (3)$$

$$\text{F1-Score} = \frac{2 \cdot \text{Precision} \cdot \text{Recall}}{\text{Precision} + \text{Recall}} \quad (4)$$

H. Experimental Results for Predicting Landslide

The LSTM model under study boasts a tri-layered structure, with each layer densely populated by 512 neurons. Despite its apparent complexity, the architecture remains streamlined and efficient, designed expressly for seamless operation on low-performance laptop hardware. The training of this model employs the AdamW optimizer, set at a learning rate of 0.0001. To ensure robustness and repeatability in our results, we conducted each experiment three times, then averaged the F1-scores, noting their standard deviation. Although the training was set for a potential maximum of 100 epochs, early stopping was incorporated with a patience of 8 epochs. Remarkably, most experiments converged to their optima around the 50 epochs. The model uses the CrossEntropyLoss function for optimization. Despite its depth and intricacy, the model remains relatively lightweight with 5.3 million trainable parameters, resulting in an estimated total model size of 21 MB. The forecast performance is depicted in Table IV.

TABLE IV. THE FORECAST PERFORMANCE OF OUR MODEL

Observed window	Forecast at	F1-score
30min	330min (∼5.5h)	0.8088 ± 0.0380
22min	292min (∼4.8h)	0.7688 ± 0.0136
22min	262min (∼4.3h)	0.7879 ± 0.0053
14min 30sec	164min 30sec (∼2.7h)	0.7927 ± 0.0319
04min 30sec	154min 30sec (∼2.5h)	0.7756 ± 0.0107
04min 30sec	124min 30sec (∼2h)	0.8232 ± 0.0122

In this research framework, the forecasting setup is delineated: The 'observed window' denotes the uninterrupted period during which data is observed. Data acquisition involved procuring three distinct time series, e.g., pressure, x-angle, and y-angle, from sensors strategically positioned on the experimental pole. The positioning strategy is squarely within the ambit of multivariate time-series forecasting [71], [72]. The forecasting objective seeks to predict events in the vicinity of the pole for a specified future time point. For example, if it monitors the three-time series for 4 minutes and 30 seconds, the predictive model aims to forecast events at the 124-minute and 30-second mark—roughly a 2-hour projection into the future.

I. Remark and Discussion

Fig. 4 illustrates the appearance of cracks on the ground, gradual soil mass horizontal displacement, and the tilted state of the sensor pile. The canal bank is progressively damaged, starting with the scour hole at the base of the slope. The canal bank is saturated after the rains and the increasing applied load. By monitoring the gradual expansion of cracks along the canal banks and around the sensor pile, the measured soil pressure data and observing the tilting behavior of the sensor pile before the soil mass ultimately failure took place over more than 12 hours. This is also identified as shown in Fig. 5 from the time the Level 1 warning signs appeared for the second time, then progressed to Level 2 warning until the soil mass slid into the canal, it took place from 21:00:00 on December 19, 2022, to 12:00:00 on December 20, 2022, equivalent to approximately 15 hours. Such behavior could be used as a signal for early warning. It should be noted that the pressure values and the behavior of tilting before failure vary case-by-case. Thus, the criteria for issuing warnings should be carefully determined.

From a research standpoint, while the F1-score demonstrates commendable performance at the 330-minute forecast time point, it is imperative to note a relatively higher standard deviation, approximately 3.8%. Our optimal prediction results are gleaned from an observational window of 4 minutes and 30 seconds to project roughly 2 hours into the future. For instance, the F1-score stands at 0.8232 with a notably low standard deviation of about 1%. However, by conducting experiments over various observational windows, we intend to establish a reliable database to provide in-depth insights for managers to implement appropriate solutions to protect the lives of residents and infrastructure.

IV. CONCLUSION

In this work, we have presented the establishment of an experimental model for monitoring the landslide of riverbank soil in the Mekong Delta region. The data collected from the experiment show good agreement with finite element method calculations. We propose warning thresholds based on soil pressure, deformation, and displacement data under saturated soil conditions. The results of this study contribute to the establishment of a system to predict the likelihood of extreme events at a specific time in the future based on 374,415 samples and three input parameters, including soil pressure, inclination of the sensor pile in directions towards and along the riverbank, warning level, and warning label, using the LSTM method. The experiment with an observation window of 4 minutes and 30 seconds indicates that the optimal result for predicting warning events is around 2 hours in the future. Through experimental results, the LSTM model effectively predicts early warning landslides for riverbanks with soft soil characteristics under external loading. The findings of this research can be applied in developing early warning systems for riverbank landslides in the Mekong Delta region.

REFERENCES

[1] P. T. T. Ngo, M. Panahi, K. Khosravi, O. Ghorbanzadeh, N. Kariminejad, A. Cerda, and S. Lee, "Evaluation of deep learning algorithms for national scale landslide susceptibility mapping of iran," *Geoscience Frontiers*, vol. 12, no. 2, pp. 505–519, 2021.

[2] M. Azarafza, M. Azarafza, H. Akgün, P. M. Atkinson, and R. Derakhshani, "Deep learning-based landslide susceptibility mapping," *Scientific reports*, vol. 11, no. 1, p. 24112, 2021.

[3] O. Ghorbanzadeh, T. Blaschke, K. Gholamnia, S. R. Meena, D. Tiede, and J. Aryal, "Evaluation of different machine learning methods and deep-learning convolutional neural networks for landslide detection," *Remote Sensing*, vol. 11, no. 2, p. 196, 2019.

[4] "Viet nam disaster and dyke ganagement authority. dong bang song cuu long: Sat lo bua vay," https://phongchongthientai.mard.gov.vn/Pages/dong-bang-song-cuu-long-sat-lo-bua-vay.aspx, (in Vietnamese).

[5] N. T. H. Diep, C. T. Nguyen, P. K. Diem, N. X. Hoang, and A. A. Kafy, "Assessment on controlling factors of urbanization possibility in a newly developing city of the vietnamese mekong delta using logistic regression analysis," *Physics and Chemistry of the Earth, Parts A/B/C*, vol. 126, p. 103065, 2022.

[6] L. T. Phat, D. V. Duy, C. T. Hieu, N. T. An, K. Lavane, and T. V. Ty, "Initial assessment on the causes of riverbank instability in chau thanh district, hau giang province," *Tap chi Khi tuong Thuy van*, vol. 740, pp. 57–73, 2022.

[7] L. X. Tu, T. B. Hoang, V. Q. Thanh, D. P. Wright, A. T. Hansan, and D. T. Anh, "Evaluation of coastal protection strategy and proposing multiple lines of defense under climate change of the mekong delta for sustainable shoreline protection," *Ocean and Coastal Management*, vol. 228, p. 106301, 2022.

[8] A. Xing, G. Wang, B. Li, Y. Jiang, Z. Feng, and T. Kamai, "Long-runout mechanism and landsliding behaviour of large catastrophic landslide triggered by heavy rainfall in guanling, guizhou, china," *Canadian Geotechnical Journal*, vol. 52, no. 7, pp. 971–981, 2015.

[9] J. Zhuang, J. Peng, G. Wang, I. Javed, Y. Wang, and W. Li, "Distribution and characteristics of landslide in loess plateau: A case study in shaanxi province," *Engineering Geology*, vol. 236, pp. 89–96, 2018.

[10] S. Xu and R. Niu, "Displacement prediction of baijiabao landslide based on empirical mode decomposition and long short-term memory neural network in three gorges area, china," *Computers & geosciences*, vol. 111, pp. 87–96, 2018.

[11] P. Reichenbach, M. Rossi, B. Malamud, M. Mihir, and F. Guzzetti, "A review of statistically-based landslide susceptibility models," *Earth-science reviews*, vol. 180, pp. 60–91, 2018.

[12] E. Sevgen, S. Kocaman, H. A. Nefeslioglu, and C. Gokceoglu, "A novel performance assessment approach using photogrammetric techniques for landslide susceptibility mapping with logistic regression, ann and random forest," *Sensors*, vol. 19, no. 18, p. 3940, 2019.

[13] M. I. Sameen, B. Pradhan, and S. Lee, "Application of convolutional neural networks featuring bayesian optimization for landslide susceptibility assessment," *Catena*, vol. 186, p. 104249, 2020.

[14] D. Sun, H. Wen, D. Wang, and J. Xu, "A random forest model of landslide susceptibility mapping based on hyperparameter optimization using bayes algorithm," *Geomorphology*, vol. 362, p. 107201, 2020.

[15] M. Conforti and F. Ietto, "Modeling shallow landslide susceptibility and assessment of the relative importance of predisposing factors, through a gis-based statistical analysis," *Geosciences*, vol. 11, no. 8, p. 333, 2021.

[16] Y. Wang, Z. Fang, and H. Hong, "Comparison of convolutional neural networks for landslide susceptibility mapping in yanshan county, china," *Science of the total environment*, vol. 666, pp. 975–993, 2019.

[17] L. Bragagnolo, R. da Silva, and J. Grzybowski, "Artificial neural network ensembles applied to the mapping of landslide susceptibility," *Catena*, vol. 184, p. 104240, 2020.

[18] C. Yu and J. Chen, "Landslide susceptibility mapping using the slope unit for southeastern helong city, jilin province, china: a comparison of ann and svm," *Symmetry*, vol. 12, no. 6, p. 1047, 2020.

[19] S. L. Ullo, A. Mohan, A. Sebastianelli, S. E. Ahamed, B. Kumar, R. Dwivedi, and G. R. Sinha, "A new mask r-cnn-based method for improved landslide detection," *IEEE Journal of Selected Topics in Applied Earth Observations and Remote Sensing*, vol. 14, pp. 3799–3810, 2021.

[20] T. Liu, T. Chen, R. Niu, and A. Plaza, "Landslide detection mapping employing cnn, resnet, and densenet in the three gorges reservoir, china," *IEEE Journal of Selected Topics in Applied Earth Observations and Remote Sensing*, vol. 14, pp. 11 417–11 428, 2021.

[21] W. L. Hakim, F. Rezaie, A. S. Nur, M. Panahi, K. Khosravi, C.-W. Lee, and S. Lee, "Convolutional neural network (cnn) with metaheuristic optimization algorithms for landslide susceptibility mapping in icheon, south korea," *Journal of environmental management*, vol. 305, p. 114367, 2022.

[22] M. Marjanović, B. Bajat, B. Abolmasov, and M. Kovaćević Marjanović, "Machine learning and landslide assessment in a gis environment," *GeoComputational Analysis and Modeling of Regional Systems*, vol. 19, no. 18, pp. 191–213, 2018.

[23] S. N. Selamat, N. A. Majid, and A. M. Taib, "A comparative assessment of sampling ratios using artificial neural network (ann) for landslide predictive model in langat river basin, selangor, malaysia," *Sustainability*, vol. 15, p. 861, 2023.

[24] H. Masruroh, A. S. Leksono, S. Kurniawan, and Soemarno, "Developing landslide susceptibility map using artificial neural network (ann) method for mitigation of land degradation," *Journal of Degraded and Mining Lands Management*, vol. 10, no. 3, pp. 4479–4494, 2023.

[25] F. Abbas, F. Zhang, F. Abbas, M. Ismail, J. Iqbal, D. Hussain, G. Khan, A. F. Alrefaei, and M. F. Albeshr, "Landslide susceptibility mapping: Analysis of different feature selection techniques with artificial neural network tuned by bayesian and metaheuristic algorithms," *Remote Sens*, vol. 15, p. 4330, 2023.

[26] M. Daviran, M. Shamekhi, R. Ghezelbash, and A. Maghsoudi, "Landslide susceptibility prediction using artificial neural networks, svms and random forest: hyperparameters tuning by genetic optimization algorithm," *International Journal of Environmental Science and Technology*, vol. 20, no. 1, pp. 259–276, 2023.

[27] S. Saha, A. Arabameri, A. Saha, T. Blaschke, P. T. T. Ngo, V. H. Nhu, and S. S. Band, "Prediction of landslide susceptibility in rudraprayag, india using novel ensemble of conditional probability and boosted regression tree-based on cross-validation method," *Science of the total environment*, vol. 764, p. 142928, 2021.

[28] Q. Zhu, A. Arabameri, M. Santosh, J. Egbueri, and J. Agbasi, "Integrated assessment of landslide susceptibility in the kalaleh basin, golestan province, iran using novel svr-goa ensemble validated with brt, ann, and elastic net models," *Environmental Science and Pollution Research*, 2023.

[29] G. Teza, S. Cola, L. Brezzi, and A. Galgaro, "Wadenow: A matlab toolbox for early forecasting of the velocity trend of a rainfall-triggered landslide by means of continuous wavelet transform and deep learning," *Geosciences*, vol. 12, p. 205, 2022.

[30] Y. Liu, G. Teza, L. Nava, Z. Chang, M. Shang, D. Xiong, and S. Cola1, "Deformation evaluation and displacement forecasting of baishuihe landslide after stabilization based on continuous wavelet transform and deep learning," *Under Review at Natural Hazards*, 2023.

[31] M. Krkac, S. B. Gazibara, Z. Arbanas, M. Secanj, and S. M. Arbanas, "A comparative study of random forests and multiple linear regression in the prediction of landslide velocity," *Landslides*, vol. 17, p. 2515–2531, 2020.

[32] V.-H. Dang, N.-D. Hoang, L.-M.-D. Nguyen, D. T. Bui, and P. Samui, "A novel gis-based random forest machine algorithm for the spatial prediction of shallow landslide susceptibility," *Forests*, vol. 11, no. 1, p. 118, 2020.

[33] D. Sun, H. Wen, D. Wang, and J. Xu, "A random forest model of landslide susceptibility mapping based on hyperparameter optimization using bayes algorithm," *Geomorphology*, vol. 362, p. 107201, 2020.

[34] B. Shi, T. Zeng, C. Tang, L. Zhang, Z. Xie, G. Lv, and Q. Wu, "Landslide risk assessment using granular fuzzy rule-based modeling: A case study on earthquake-triggered landslides," *IEEE Access*, vol. 9, pp. 135 790–135 802, 2021.

[35] S. Badola, V. N. Mishra, S. Parkash, and M. Pandey, "Rule-based fuzzy inference system for landslide susceptibility mapping along national highway 7 in garhwal himalayas, india," *Quaternary Science Advances*, vol. 11, p. 107201, 2023.

[36] A. Aggarwal, M. Alshehri, M. Kumar, O. Alfarraj, P. Sharma, and K. R. Pardasani, "Landslide data analysis using various time-series forecasting models," *Computers & Electrical Engineering*, vol. 88, p. 106858, 2020.

[37] L. Xiao, Y. Zhang, and G. Peng, "Landslide susceptibility assessment using integrated deep learning algorithm along the china-nepal highway," *Sensors*, vol. 18, no. 12, p. 4436, 2018.

[38] P. Xie, A. Zhou, and B. Chai, "The application of long short-term memory(lstm) method on displacement prediction of multifactor-induced landslides," *IEEE Access*, vol. 7, pp. 54 305–54 311, 2019.

[39] S. Xu and R. Niu, "Displacement prediction of baijiabao landslide based on empirical mode decomposition and long short-term memory neural network in three gorges area, china," *Computers and geosciences*, vol. 111, pp. 87–96, 2018.

[40] H. Jiang, Y. Li, C. Zhou, H. Hong, T. Glade, and K. Yin, "Landslide displacement prediction combining lstm and svr algorithms: A case study of shengjibao landslide from the three gorges reservoir area," *Applied Sciences*, vol. 10, no. 21, p. 7830, 2020.

[41] X. Zhang, C. Zhu, M. He, M. Dong, G. Zhang, and F. Zhang, "Failure mechanism and long short-term memory neural network model for landslide risk prediction," *Remote Sensing*, vol. 14, no. 1, p. 166, 2021.

[42] H. Shafizadeh-Moghadam, R. Valavi, H. Shahabi, K. Chapi, and A. Shirzadi, "Novel forecasting approaches using combination of machine learning and statistical models for flood susceptibility mapping," *Journal of environmental management*, vol. 217, pp. 1–11, 2018.

[43] K. Khosravi, H. Shahabi, B. T. Pham, J. Adamowski, A. Shirzadi, B. Pradhan, J. Dou, H.-B. Ly, G. Gróf, H. L. Ho, H. Hong, K. Chapi, and I. Prakash, "A comparative assessment of flood susceptibility modeling using multi-criteria decision-making analysis and machine learning methods," *Journal of Hydrology*, vol. 573, pp. 311–323, 2019.

[44] O. Rahmati, M. Panahi, Z. Kalantari, E. Soltani, F. Falah, K. S. Dayal, F. Mohammadi, R. C. Deo, J. Tiefenbacher, and D. T. Bui, "Capability and robustness of novel hybridized models used for drought hazard modeling in southeast queensland, australia," *Science of The Total Environment*, vol. 718, p. 134656, 2020.

[45] H. Li, Q. Xu, Y. He, X. Fan, H. Yang, and S. Li, "Temporal detection of sharp landslide deformation with ensemble-based lstm-rnns and hurst exponent," *Geomatics, Natural Hazards and Risk*, vol. 12, no. 1, pp. 3089–3113, 2021.

[46] Y. Dai, W. Dai, W. Yu, and D. Bai, "Determination of landslide displacement warning thresholds by applying dba-lstm and numerical simulation algorithms," *Applied Sciences*, vol. 12, no. 13, p. 6690, 2022.

[47] B. Yang, K. Yin, S. Lacasse, and Z. Liu, "Time series analysis and long short-term memory neural network to predict landslide displacement," *Landslides*, vol. 16, pp. 677–694, 2019.

[48] Y. Xing, J. Yue, and C. Chen, "Interval estimation of landslide displacement prediction based on time series decomposition and long short-term memory network," *IEEE Access*, vol. 8, pp. 3187–3196, 2019.

[49] J. Li, W. Wang, and Z. Han, "A variable weight combination model for prediction on landslide displacement using ar model, lstm model, and svm model: a case study of the xinming landslide in china," *Environmental Earth Sciences*, vol. 80, no. 10, p. 386, 2021.

[50] Y. Gao, X. Chen, R. Tu, G. Chen, T. Luo, and D. Xue, "Prediction of landslide displacement based on the combined vmd-stacked lstm-tar model," *Remote Sensing*, vol. 14, no. 5, p. 1164, 2022.

[51] Z. Lin, X. Sun, and Y. Ji, "Landslide displacement prediction model using time series analysis method and modified lstm model," *Electronics*, vol. 11, no. 10, p. 1519, 2022.

[52] S. Yang, A. Jin, W. Nie, C. Liu, and Y. Li, "Research on ssa-lstm-based slope monitoring and early warning model," *Sustainability*, vol. 14, no. 16, p. 10246, 2022.

[53] E. A. Oguz, I. Depina, B. Myhre, G. Devoli, H. Rustad, and V. Thakur, "Iot-based hydrological monitoring of water-induced landslides: a case study in central norway," *Bulletin of Engineering Geology and the Environment*, vol. 81, no. 5, p. 217, 2022.

[54] A. Joshi, J. Grover, D. P. Kanungo, and R. K. Panigrahi, "Edge assisted reliable landslide early warning system," *In 2019 IEEE 16th India Council International Conference (INDICON)*, pp. 1–4, 2019.

[55] M. Gamperl, J. Singer, and K. Thuro, "Internet of things geosensor network for cost-effective landslide early warning systems," *Sensors*, vol. 21, no. 8, p. 2609, 2021.

[56] M. T. Abraham, N. Satyam, B. Pradhan, and A. M. Alamri, "Iot-based geotechnical monitoring of unstable slopes for landslide early warning in the darjeeling himalayas," *Sensors*, vol. 20, no. 9, p. 2611, 2022.

[57] C. Wang, W. Guo, K. Yang, and X. Wang, "Real-time monitoring system of landslide based on lora architecture," *Frontiers in Earth Science*, vol. 10, p. 899509, 2022.

[58] D. El Houssaini, S. Khriji, C. Viehweger, T. Keutel, and O. Kanoun, "Location-aware iot-enabled wireless sensor networks for landslide early warning," *Electronics*, vol. 11, no. 23, p. 3971, 2022.

[59] L. Piciullo, V. Capobianco, and H. Heyerdahl, "A first step towards a iot-based local early warning system for an unsaturated slope in norway," *Natural Hazards*, vol. 114, no. 3, pp. 3377–3407, 2022.

[60] Q. A. Gian, D. T. Tran, D. C. Nguyen, V. H. Nhu, and D. T. Bui, "Design and implementation of site-specific rainfall-induced landslide early warning and monitoring system: a case study at nam dan landslide (vietnam)," *Geomatics, Natural Hazards and Risk*, vol. 8, no. 2, pp. 1978–1996, 2017.

[61] T. V. Ty, P. H. Tien, L. V. Thinh, H. T. C. Hong, C. N. Thang, D. V. Duy, N. T. An, L. Q. Anh, and N. T. Liem, "Phan tich cac yeu to anh huong den on dinh bo song: truong hop nghien cuu tai doan song cha va, tinh vinh long," *Tap chi Khoa hoc Dai hoc can Tho*, vol. 58, no. 5, pp. 14–21, 2022 (Vietnamese).

[62] P. K. Diem, D. V. Den, V. Q. Minh, and N. T. H. Diep, "Danh gia tinh hinh sat lo, boi tu khu vuc ven bien tinh ca mau va bac lieu tu 1995-2010 su dung vien tham va cong nghe gis," *Tap chi Khoa hoc Dai hoc can Tho*, no. 26, pp. 35–43, 2013 (Vietnamese).

[63] H. D. Khoa, H. T. C. Hong, T. N. Thanh, N. T. T. Lieu, T. V. Ty, C. Than, C. N. Thang, H. T. Toan, H. T. Minh, D. V. Duy, and T. Q. Ninh, "Quan trac dien bien duong bo cu lao dung bang cong nghe phan tich anh vien tham," *Tap chi Vat lieu and Xay dung-Bo Xay dung*, vol. 13, no. 2, pp. 54–58, 2023 (Vietnamese).

[64] N. T. H. Diep, N. T. Loi, and N. T. Can, "Monitoring erosion and accretion situation in the coastal zone at kien giang province," *The International Archives of the Photogrammetry, Remote Sensing and Spatial Information Sciences*, no. 42, pp. 197–203, 2018.

[65] "Natural resources and environment newspaper. sat lo bo song, xoi lo bo bien - van de nhuc nhoi cua dong bang song cuu long," https://baotainguyenmoitruong.vn/satlobosongxoilobobienvandenhucnhoicuadongbar (in Vietnamese).

[66] N. V. Liem, N. P. Dat, B. T. Dieu, V. V. Phai, P. T. Trinh, H. Q. Vinh, and T. V. Phong, "Assessment of geomorphic processes and active tectonics in con voi mountain range area (northern vietnam) using the hypsometric curve analysis method," *Vietnam Journal of Earth Sciences*, vol. 38, no. 2, pp. 202–216, 2016.

[67] O. Ghorbanzadeh, H. Shahabi, A. Crivellari, S. Homayouni, T. Blaschke, and P. Ghamisi, "Landslide detection using deep learning and object-based image analysis," *Landslides*, vol. 19, no. 4, pp. 929–939, 2022.

[68] A. A. Taha and A. Hanbury, "Metrics for evaluating 3d medical image segmentation: analysis, selection, and tool," *BMC medical imaging*, vol. 15, no. 1, pp. 1–28, 2015.

[69] V.-H. Nhu, A. Mohammadi, H. Shahabi, B. B. Ahmad, N. Al-Ansari, A. Shirzadi, M. Geertsema, V. R. Kress, S. Karimzadeh, K. V. Kamran, W. Chen, and H. Nguyen, "Landslide detection and susceptibility modeling on cameron highlands (malaysia): A comparison between random forest, logistic regression and logistic model tree algorithms," *Forests*, vol. 11, no. 8, p. 830, 2020.

[70] P. Yariyan, S. Janizadeh, T. Van Phong, H. D. Nguyen, R. Costache, H. Van Le, B. T. Pham, B. Pradhan, and J. P. Tiefenbacher, "Improvement of best first decision trees using bagging and dagging ensembles for flood probability mapping," *Water Resources Management*, vol. 34, pp. 3037–3053, 2020.

[71] K. Madhusudhanan, J. Burchert, N. Duong-Trung, S. Born, and L. Schmidt-Thieme, "U-net inspired transformer architecture for far horizon time series forecasting," *In: Joint European Conference on Machine Learning and Knowledge Discovery in Databases. Cham: Springer Nature Switzerland*, pp. 36–52, 2022.

[72] N. Duong-Trung, D.-M. Nguyen, and D. Le-Phuoc, "Temporal saliency detection towards explainable transformer-based timeseries forecasting," *arXiv preprint arXiv:2212.07771*, 2023.